

# Rainbow scattering in nuclear collisions

Yu. A. Berezhnoi, A. V. Kuznichenko, and G. M. Onishchenko

*A. M. Gorki State University, Kharkov*

V. V. Pilipenko

*Physicotechnical Institute, Ukrainian Academy of Sciences, Kharkov*

*Fiz. Elem. Chastits At. Yadra* **18**, 289–322 (March–April 1987)

The evolution of ideas about the rainbow phenomenon resulting from the refraction and reflection of light in water drops is briefly reviewed. The rainbow scattering of particles in quantum mechanics is treated on the basis of the semiclassical approximation, and the nuclear and Coulomb “rainbows” are discussed. Rainbow scattering of light ions by nuclei at energies  $E \gtrsim 25\text{--}30$  MeV/nucleon is considered. The results of theoretical analysis of experimental data on rainbow scattering are presented. The behavior of the nuclear part of the scattering phase shift deduced from experiment is discussed. The manifestation of rainbow scattering in quasielastic nuclear processes is considered.

## 1. THE RAINBOW PHENOMENON IN OPTICS

The rainbow is one of the most beautiful optical phenomena in the atmosphere. The phenomenon has been known since ancient times, but an explanation of its physical nature could be found only when the laws of refraction and reflection of light rays at the boundary of two media had been found. However, knowledge of the laws of geometrical optics was not sufficient for the complete description of the rainbow. The investigation of the optical rainbow required the efforts of different scientists over several centuries and is associated with the names of Roger Bacon, Maurolycus, Descartes, Newton, Fresnel, Airy, and others.<sup>1,2</sup> The modern theory of the optical rainbow requires knowledge of the phenomena of quantum optics (interference and diffraction) and the corpuscular properties of light (polarization, photon momentum). The Russian name for rainbow, *raduga*, in fact derives from the old Slavonic word *rad*, which means joyful.

At the present time, the exact mathematical description of the rainbow is based on the solution to the problem of the scattering of electromagnetic waves by conducting spheres (Mie's theory). This problem involves the solution of Maxwell's equations with appropriate boundary conditions.<sup>3,4</sup> The essence of the phenomenon of rainbow scattering can be understood by considering the path of rays in a drop of water (Fig. 1). It can be seen from the figure that the rays which emerge from a drop accumulate near the limiting angle  $\theta_{\max}$ , this leading to an increase in the intensity of the light in this region of angles.

Rainbow scattering of different particles analogous to the optical rainbow is also observed in atomic and nuclear collisions.<sup>5</sup> The analogy between the scattering of light and particles is that in rainbow scattering there is a limiting angle near which the classical trajectories (rays) accumulate, this leading to an increase in the intensity of the scattered particles near the rainbow angle.

Extensive experimental material has been accumulated on the elastic scattering of different particles by nuclei in the region of energies at which rainbow scattering is manifested. Rainbow scattering has a strong influence on the behavior of the differential cross sections in different regions of scattering angles, which are determined by the nature of the phenomenon (nuclear or Coulomb rainbow). The nuclear rain-

bow effect is manifested in the cross sections of elastic scattering of light nuclei by nuclei in the form of damping of the diffraction oscillations in the region of central angles. However, not all damping of the oscillations in the cross sections is due to rainbow scattering; other effects are at work, for example, in the scattering of sufficiently heavy ions by intermediate and heavy nuclei. The Coulomb rainbow effect changes the behavior of the cross section in the region of the Coulomb angle.

Damping of oscillations is also observed in experiments on inelastic nuclear scattering of particles with excitation of low-lying nuclear states. This effect is a manifestation of rainbow scattering in inelastic processes. Rainbow scattering is also characteristic of various quasielastic nuclear reactions. An example is the charge-exchange nuclear reaction with excitation in the final nucleus of the isobar analog of the target-nucleus ground state.

There exist at present two alternative approaches for the theoretical description of rainbow scattering. One of them is based on the optical model, while the other is associated with the description of the interaction by means of the  $S$  matrix. The analysis of rainbow scattering in nuclear processes which now follows is based on the  $S$ -matrix formalism.

## 2. RAINBOW SCATTERING IN QUANTUM MECHANICS

The wave nature of quantum-mechanical objects and the possibility of semiclassical description of scattering pro-

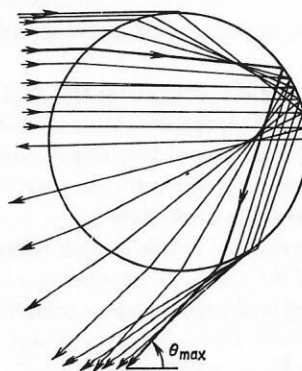


FIG. 1. Light-ray trajectories in a water drop ( $\theta_{\max}$  is the rainbow angle).

cesses at sufficiently high energies establishes a number of analogies between atomic or nuclear scattering and optics. These include Fraunhofer and Fresnel diffraction, glory (halo effect), and rainbow scattering. A detailed description of all details of these processes can be found, for example, in Refs. 4 and 6. We shall consider the basic features of quantum-mechanical rainbow scattering, using the semiclassical approximation.

We consider first the details of particle scattering in classical mechanics. The classical scattering cross section is determined by the expression

$$d\sigma_{cl}(\theta) = \frac{b}{\sin \theta} \left| \frac{db}{d\theta} \right| d\Omega,$$

where  $\theta$  is the scattering angle and  $b$  is the impact parameter. We define the classical deflection function<sup>4</sup>:

$$\Theta(b) = \pi - 2b \int_{r_{min}}^{\infty} \frac{dr}{r^2} \left[ 1 - \frac{U(r)}{E} - \frac{b^2}{r^2} \right]^{-1/2}, \quad (1)$$

where  $r_{min}$  is the distance of closest approach, determined by the vanishing of the expression in the square brackets in (1),  $E$  is the energy, and  $U(r)$  is the scattering potential.

The function  $\Theta(b)$  determines the deflection angle of particles moving along trajectories with impact parameter  $b$ . It can be seen from (1) that the function  $\Theta(b)$  takes values in the interval  $-\infty < \Theta(b) \leq \pi$ . In the case of a monotonic attractive potential,  $\Theta(b)$  is always negative; for a monotonic repulsive potential, it is always positive.

For a given scattering angle  $\theta$  ( $0 \leq \theta \leq \pi$ ) contributions to the cross section can be made by trajectories that are deflected through angles  $+\theta$  and  $-\theta$  and also by the trajectories that appear at angles  $\pm\theta$  after passing round the scattering center several times, i.e.,

$$\Theta(b) = \pm\theta - 2\pi m, \quad m = 0, 1, 2, \dots \quad (2)$$

Negative values of  $m$  are not encountered, since deflection by an angle exceeding  $\pi$  is dynamically impossible.

Bearing in mind that  $db/d\theta = 1/\Theta'(b)$ , we represent the classical scattering cross section in the form

$$d\sigma_{cl}(\theta) = \frac{b}{\sin \theta} \frac{1}{|\Theta'(b)|} d\Omega. \quad (3)$$

In many cases (for example, for a monotonic regular attractive potential) the inversion of the deflection function  $\Theta(b)$  is not unique, i.e., to each scattering angle  $\theta$  there correspond two or more impact parameters  $b$ , and the deflection function can have extrema. If an extremum occurs for impact parameter  $b_r$ , then  $\Theta'(b_r) = 0$ , and in the classical scattering cross section a singularity appears at the corresponding angle  $\theta_r = |\Theta(b_r)|$ .

If  $\theta_r \neq 0$  and  $\theta_r \neq \pi$ , then the scattering near the angle  $\theta_r$  is called rainbow scattering, and  $\theta_r$  is called the rainbow angle. In accordance with (3), the classical scattering cross section becomes infinite as  $\theta \rightarrow \theta_r - 0$ , since the density of the emerging trajectories then becomes infinitely large. For scattering angles exceeding the maximal rainbow angle there are no classical trajectories, and the classical cross section is zero. Strong attraction capable of leading to rainbow scattering can occur in nuclear collisions. The possibility of rainbow scattering for microscopic objects was first predicted by Kenneth Ford and John Wheeler.<sup>5</sup>

In the quantum-mechanical treatment, the cross section does not become infinite at the angle  $\theta = \theta_r$  and is not equal to zero in the classically inaccessible region  $\theta > \theta_r$ . We shall consider in more detail the scattering process at angles near  $\theta_r$  in the framework of the semiclassical approximation.

We represent the scattering amplitude in the form of a partial-wave expansion,

$$f(\theta) = \frac{1}{2ik} \sum_{l=0}^{\infty} (2l+1) [S_l - 1] P_l(\cos \theta), \quad (4)$$

where  $k$  is the wave vector,  $S_l$  is the  $S$ -matrix element in the angular-momentum representation, and  $P_l(\cos \theta)$  is a Legendre polynomial.

In  $S_l$  we separate the modulus  $\eta_l$  and phase  $\delta_l$ :

$$S_l = \eta_l e^{2i\delta_l}.$$

For a real potential,  $\eta_l = 1$  for all  $l$ . If there is absorption (complex potential), then  $\eta_l < 1$  for a certain interval of  $l$  values.

If the energy of the colliding particles is sufficiently high, then in (4) it is possible to go over from summation to integration. Such a transition is usually made by means of various summation formulas (for example, the formulas of Ostrogradskii, Poisson, and others). Using Poisson's summation formula and also replacing the Legendre polynomials in (4) by their asymptotic behavior at large  $l$ ,

$$P_l(\cos \theta) \approx \frac{1}{\sqrt{\pi(2l+1)\sin \theta}} \left\{ \exp \left[ i \left( l + \frac{1}{2} \right) \theta - i \frac{\pi}{4} \right] + \exp \left[ -i \left( l + \frac{1}{2} \right) \theta + i \frac{\pi}{4} \right] \right\},$$

$$\frac{1}{l} \ll \theta \ll \pi - \frac{1}{l},$$

we obtain for the scattering amplitude the expression<sup>6,7</sup>

$$f(\theta) = \frac{1}{ik\sqrt{2\pi\sin \theta}} \sum_{m=-\infty}^{\infty} (-1)^m \int_0^{\infty} dL L^{1/2} \eta(L) [e^{iA_m^+(L, \theta)} + e^{-iA_m^-(L, \theta)}], \quad (5)$$

where we have introduced the notation

$$A_m^{\pm}(L, \theta) = \frac{\pi}{4} - L\theta \pm 2\pi m L \pm \delta(L), \quad L = l + \frac{1}{2}.$$

In (5), we have omitted the terms corresponding to the unity in the square brackets in Eq. (4), since it contributes only to the scattering at zero angle.

Suppose that the scattering process takes place under semiclassical conditions and involves a large number of partial waves. We consider the case of weak absorption and assume that  $\eta(L)$  is a slowly-varying function. Then contributions to the integrals in (5) are made only by the neighborhoods of the points of stationary phase  $L_s$ , which are determined by the relations

$$\frac{dA_m^{\pm}(L, \theta)}{dL} = -\theta \pm 2\pi m \pm 2 \frac{d\delta(L)}{dL} = 0. \quad (6)$$

The transition from quantum to classical mechanics corresponds to the substitution

$$l(l+1) \approx \left( l + \frac{1}{2} \right)^2 \rightarrow (kb)^2. \quad (7)$$

Bearing in mind that in the WKB approximation the semiclassical phase shift  $\delta_{cl}(L)$  is determined by the expression

$$\delta_{cl}(L) = \frac{\pi L}{2} - k \int_{r_{min}}^{\infty} dr r \left[ \frac{d}{dr} \sqrt{1 - \frac{U(r)}{E} - \frac{L^2}{k^2 r^2}} \right],$$

we obtain

$$2 \frac{d\delta_{cl}(L)}{dL} = \pi - \frac{2L}{k} \int_{r_{min}}^{\infty} \frac{dr}{r^2} \left[ 1 - \frac{U(r)}{E} - \frac{L^2}{k^2 r^2} \right]^{-1/2}. \quad (8)$$

Replacing  $L = 1 + \frac{1}{2}$  in (7) by  $kb$ , we see that the right-hand side of Eq. (8) is equal to the classical deflection function (1). Therefore, the deflection function can be related to the phase shift:

$$\Theta(L) = 2d\delta(L)/dL. \quad (9)$$

The expression (9) is the definition of the quantum deflection function. The equation for finding the stationary points (6) takes the same form as the classical equation (2). Thus, the stationary points determined in accordance with (6) correspond to motion in classical trajectories that lead to scattering of the particle by angle  $\theta$ . The terms in (5) with nonzero  $m$  correspond in the semiclassical sense to the situation when the particle makes several revolutions around the scattering center.<sup>6</sup> In some cases, these terms may make an appreciable contribution to the scattering cross section. Such a situation occurs if the deflection function  $\Theta(L)$  exceeds  $\pi$  in absolute value and the corresponding contribution is not suppressed by the presence of strong absorption. These terms may also make appreciable corrections in the presence of strong absorption with a sharp boundary.<sup>7</sup> However, for real interactions of light and heavy ions with nuclei in the region of intermediate energies it is as a rule sufficient when studying the behavior of the differential cross sections to restrict oneself in (5) to the term with  $m = 0$ . Corresponding estimates show that the terms then ignored are small compared with the main retained term.<sup>7-9</sup> Therefore, in what follows we shall use for the scattering amplitude the expression

$$f(\theta) = \frac{1}{ik \sqrt{2\pi \sin \theta}} \int_0^{\infty} \eta(L) [e^{iA_0^+(L, \theta)} + e^{-iA_0^-(L, \theta)}] L^{1/2} dL. \quad (10)$$

The amplitude (10) consists of two parts. The part containing  $A_0^+(L, \theta)$  is called the nearside amplitude, and the part containing  $A_0^-(L, \theta)$  the farside amplitude, this being done in accordance with their semiclassical significance (scattering from the near and far edges of the scatterer). The division into the nearside and farside amplitudes is often helpful for qualitative analysis of the behavior of the differential cross section.<sup>10,11</sup>

We now consider the scattering of charged particles for which there is a weak attraction in addition to the Coulomb interaction. The deflection function  $\Theta(L)$  is monotonic, positive, and decreases smoothly from the value  $\pi$  at  $L = 0$  to zero at  $L = \infty$ . The typical behavior of the function  $\Theta(L)$  is shown in Fig. 2. In this situation, only one point of stationary phase  $L_s$ , which is contained in the nearside amplitude and is determined by the condition  $\Theta(L_s) = \theta$ , makes a contribution.

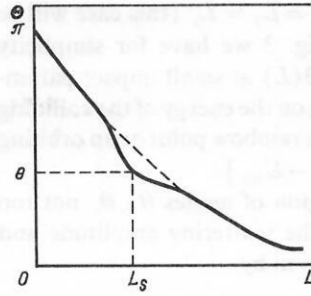


FIG. 2. Deflection angle in the presence of Coulomb repulsion and weak attraction ( $L_s$  is the stationary point corresponding to the scattering angle  $\theta$ ).

We expand  $A_0^+(L, \theta)$  in a series near the stationary point up to terms of second order:

$$A_0^+(L, \theta) = \frac{\pi}{4} - L_s \theta + 2\delta(L_s) + \frac{1}{2} \Theta'(L_s) (L - L_s)^2. \quad (11)$$

In (10), we ignore the contribution of the farside amplitude [the term with  $A_0^-(L, \theta)$ ] and substitute the expansion (11) in (10). Extending the integration in (10) at the lower limit to  $-\infty$ , we obtain for the amplitude and differential scattering cross section the expressions

$$f(\theta) = \frac{1}{k} \sqrt{\frac{L_s}{\sin \theta}} \frac{\eta(L_s)}{\sqrt{\Theta'(L_s)}} e^{i[2\delta(L_s) - L_s \theta]};$$

$$d\sigma(\theta) = \frac{L_s}{k^2 \sin \theta} \frac{1}{|\Theta'(L_s)|} \eta^2(L_s) d\Omega.$$

Replacing  $L_s$  by  $kb$  and bearing in mind that  $\Theta'(L_s) = \Theta'(b)/k$ , we obtain

$$d\sigma(\theta) = \frac{b}{\sin \theta} \frac{P(b)}{|\Theta'(b)|} d\Omega. \quad (12)$$

The cross section (12) differs from the classical cross section (3) only by the suppression factor  $P(b)$ , which is equal to

$$P(b) = \eta^2(kb) \leq 1.$$

We now suppose that at short distances between the charged particles there is a fairly strong attraction. The presence of strong attraction leads to a significant deviation in the behavior of the deflection function  $\Theta(L)$  from the purely Coulomb function, a deep dip into the region of negative values being formed in it at small impact parameters. In this case, the deflection function  $\Theta(L)$  is nonmonotonic, and there are several stationary points in the integrand in (10). We consider as an example the deflection function  $\Theta(L)$  in Fig. 3. The deflection function shown there has two stationary points  $L_1$  and  $L_2$  for  $\theta < \theta_r$ . For  $\theta = \theta_r$ , the two station-

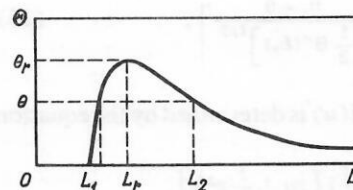


FIG. 3. Deflection angle in the presence of Coulomb repulsion and strong attraction [ $L_1$  and  $L_2$  are the stationary points corresponding to the scattering angle  $\theta$ ,  $L_r$  is the rainbow point (Coulomb rainbow), and  $\theta_r$  is the rainbow angle].

any points merge into one:  $L_1 = L_2 = L_r$  (this case will be considered separately). In Fig. 3 we have for simplicity omitted the negative part of  $\Theta(L)$  at small impact parameters. In this region, depending on the energy of the colliding particles, there may also exist a rainbow point or an orbiting point  $L_{orb}$  [ $\Theta(L) \rightarrow -\infty$  as  $L \rightarrow L_{orb}$ ].

We consider first the region of angles  $\theta < \theta_r$  not too close to the rainbow angle. The scattering amplitude and cross section in this case are given by

$$f(\theta) = \frac{1}{k} \sqrt{\frac{L_1}{\sin \theta}} \frac{\eta(L_1)}{\sqrt{\Theta'(L_1)}} e^{i[2\delta(L_1) - L_1\theta]} + \frac{1}{k} \sqrt{\frac{L_2}{\sin \theta}} \frac{\eta(L_2)}{\sqrt{\Theta'(L_2)}} e^{i[2\delta(L_2) - L_2\theta]}, \quad (13)$$

$$\sigma(\theta) = \frac{1}{k^2 \sin \theta} \left\{ \left| \frac{L_1}{\Theta'(L_1)} \right| \eta^2(L_1) + \left| \frac{L_2}{\Theta'(L_2)} \right| \eta^2(L_2) - 2 \sqrt{\frac{L_1 L_2}{|\Theta'(L_1) \Theta'(L_2)|}} \eta(L_1) \eta(L_2) \sin [2\delta(L_1) - 2\delta(L_2) + (L_2 - L_1)\theta] \right\}, \quad (14)$$

where  $\sigma(\theta) = d\sigma(\theta)/d\Omega$ .

The last expression differs from the classical cross section for the deflection function given in Fig. 3 by the interference term, which vanishes only on averaging over a sufficiently large region of angles containing many oscillations.

When the scattering angle tends to the rainbow angle,  $\theta \rightarrow \theta_r$ , the approximation used in the derivation of the expression (13) becomes invalid, since  $\Theta'(L_r) = 0$ . We note that then the cross section in (14), like the classical cross section, tends to infinity. In the case of coincidence of the two stationary points,  $L_1 = L_2 = L_r$ , a stationary point of higher order arises. Therefore, the function  $A_0^+(L, \theta)$  near the point  $L_r$  must be expanded in a series up to the terms of third order. Bearing in mind that  $\Theta(L_r) = \theta_r$ , we obtain

$$A_0^+(L, \theta) \approx \frac{\pi}{4} - L_r\theta + 2\delta(L_r) + (L - L_r)(\theta_r - \theta) + \frac{1}{6}(L - L_r)^3 \Theta''(L_r).$$

The scattering amplitude is now

$$f(\theta) \approx \frac{1}{k} \sqrt{\frac{L_r}{2\pi \sin \theta}} \exp \left\{ i \left[ 2\delta(L_r) - L_r\theta - \frac{\pi}{4} \right] \right\} \times \int_{-\infty}^{\infty} dL \eta(L) \exp \left\{ i \left[ (\theta_r - \theta)(L - L_r) + \frac{1}{6} \Theta''(L_r)(L - L_r)^3 \right] \right\}.$$

As before, we assume that  $\eta(L)$  is a slowly varying function. Therefore,

$$f(\theta) = \frac{1}{k} \sqrt{\frac{2\pi L_r}{\sin \theta}} \left[ \frac{2}{\Theta''(L_r)} \right]^{1/3} \eta(L_r) \exp \left\{ i \left[ 2\delta(L_r) - L_r\theta - \frac{\pi}{4} \right] \right\} \times \text{Ai} \left[ \frac{\theta_r - \theta}{\left[ \frac{1}{2} \Theta''(L_r) \right]^{1/3}} \right], \quad (15)$$

where the Airy function  $\text{Ai}(u)$  is determined by the equation

$$\text{Ai}(u) = \frac{1}{2\pi} \int_{-\infty}^{\infty} dx \exp \left[ i \left( xu + \frac{1}{3} x^3 \right) \right].$$

The cross section of scattering through angles near  $\theta_r$  is determined by the expression

$$\sigma(\theta) = \frac{2\pi L_r \eta^2(L_r)}{k^2 \sin \theta} \left[ \frac{2}{\Theta''(L_r)} \right]^{2/3} \left[ \text{Ai} \left[ \frac{\theta_r - \theta}{\left[ \frac{1}{2} \Theta''(L_r) \right]^{1/3}} \right] \right]^2, \quad (16)$$

The cross section (16) has the same form as the corresponding expression in optics<sup>4</sup> and is called the Airy approximation to rainbow scattering. As  $u \rightarrow \pm \infty$ , the Airy function  $\text{Ai}(u)$  has the asymptotic behavior

$$\text{Ai}(u) \approx \begin{cases} (-\pi^2 u)^{-1/4} \cos \left[ \frac{2}{3} (-u)^{3/2} - \frac{\pi}{4} \right], & u \rightarrow -\infty; \\ \frac{1}{2} (\pi^2 u)^{-1/4} \exp \left( -\frac{2}{3} u^{3/2} \right), & u \rightarrow \infty. \end{cases} \quad (17)$$

The cross section (16) is bounded at  $\theta = \theta_r$ , since the function  $\text{Ai}(0)$  is finite, though it does have a maximum in the region of negative arguments near zero. The cross section (16) decreases smoothly when  $\theta > \theta_r$  (shadowed region), while for  $\theta < \theta_r$  (illuminated region) it oscillates, this corresponding to the main and subsidiary arcs of the rainbow in optics.

In the region of angles  $\theta > \theta_r$  far from  $\theta_r$ , the cross section is again determined by an isolated stationary point of first order, which, however, is now complex,<sup>12</sup> and this leads to an exponential decrease of the cross section.

Hitherto, we have not made any assumptions about the absorption of the scattered waves, i.e., we have considered the case of weak absorption. However, in quantum-mechanical problems one must frequently study cases with strong absorption (especially in the case of hadron collisions with nuclei). It is therefore important to establish how the presence of strong absorption affects the nature of the scattering.

We shall assume that in the scattering all the partial waves with  $L < L_0$  are completely absorbed, while the waves with  $L > L_0$  pass completely through the scatterer (model of a sharp absorption boundary). Therefore, we have

$$\eta(L) = \begin{cases} 0, & L < L_0; \\ 1, & L > L_0. \end{cases} \quad (18)$$

In reality, the function  $\eta(L)$  usually varies smoothly from zero to unity in the region of the limiting angular momentum  $L_0$ . However, the function  $\eta(L)$  in (18) can be used to study the qualitative behavior of the cross section.

In connection with the strong absorption of waves with  $L < L_0$ , all the details of the scattering are related to the behavior of the deflection function  $\Theta(L)$  in the region  $L > L_0$ . In particular, in the case of strong attraction leading to the appearance of a rainbow point the part of the deflection function shown in Fig. 3 is important. The behavior of  $\Theta(L)$  at small angular momenta can be important only if there is at least a small transparency for waves with small  $L$ . The rainbow point shown in Fig. 3 is called the Coulomb rainbow. The phenomenon of the Coulomb rainbow, historically the first example of rainbow scattering in nuclear collisions, was considered for the scattering of  $\alpha$  particles of relatively low energies by nuclei.<sup>5,13</sup> The presence of the Coulomb rainbow has a significant influence on the cross section when the Coulomb interaction between the colliding particles is large, as is the case for the scattering of heavy ions by nuclei. It is this case that we consider below.

We consider first the case of weak attraction (see Fig. 2). Using again the method of stationary phase, we obtain for the scattering amplitude the expression

$$f(\theta) = -\frac{i}{k} \sqrt{\frac{L_s}{2\pi \sin \theta}} \exp \left\{ i \left[ 2\delta(L_s) - L_s \theta + \frac{\pi}{4} \right] \right\} \\ \times \int_{L_0}^{\infty} dL \exp \left[ -\frac{i}{2} \Theta'(L_s) (L - L_s)^2 \right].$$

Defining the (complementary) error function by the relation

$$\operatorname{erfc}(t) = \frac{2}{\sqrt{\pi}} \int_t^{\infty} e^{-x^2} dx,$$

we find<sup>6</sup>

$$f(\theta) = \frac{1}{2k} \sqrt{\frac{L_s}{\sin \theta}} \frac{e^{i[2\delta(L_s) - L_s \theta]}}{\sqrt{\Theta'(L_s)}} \\ \times \operatorname{erfc} \left[ e^{-i\frac{\pi}{4}} \sqrt{\frac{1}{2} \Theta'(L_s) (L_0 - L_s)} \right]. \quad (19)$$

In (19), no allowance is made for the Fraunhofer part of the amplitude associated with the contribution to  $f(\theta)$  from the limit point  $L_0$ . This correction may lead in the considered case to the appearance of Fraunhofer oscillations in the region of large scattering angles.

The differential cross section is now

$$\sigma(\theta) = \frac{L_s}{k^2 \sin \theta} \frac{1}{|\Theta'(L_s)|} \\ \times \left| \frac{1}{2} \operatorname{erfc} \left[ e^{-i\frac{\pi}{4}} \sqrt{\frac{1}{2} |\Theta'(L_s)| (L_0 - L_s)} \right] \right|^2. \quad (20)$$

It is readily seen that the cross section (20) again differs from the classical cross section (3) only by a suppression factor

$$P = \left| \frac{1}{2} \operatorname{erfc} \left[ e^{-i\frac{\pi}{4}} \sqrt{\frac{1}{2} |\Theta'(L_s)| (L_0 - L_s)} \right] \right|^2.$$

However, in contrast to weak absorption, the suppression factor now leads to oscillations in the illuminated region  $\theta < \theta_0$ . The angle  $\theta_0$  corresponds to the limiting angular momentum  $L_0$  and is determined by the relation  $\theta_0 = \Theta(L_0)$ . In the shadowed region  $\theta > \theta_0$ , the factor  $P$  leads to rapid decrease of the cross section (20).

Finally, we consider the scattering of charged particles in the presence of strong attraction and strong absorption with the deflection function shown in Fig. 3. The investigation of this case is particularly important for understanding the interaction of heavy ions with nuclei. In the region of angles  $\theta < \theta_r$  there are two stationary points  $L_1$  and  $L_2$ , which make contributions analogous to (19) to the amplitude. If the difference  $L_1 - L_0$  is sufficiently large, the two stationary points make comparable contributions to the cross section. But if  $L_0 \gtrsim L_1$ , then  $L_1$  lies in the shadowed region and the contribution from it to the cross section is small because of the presence of the strong absorption. Therefore, we shall ignore the contribution from the point  $L_1$ . The stationary point  $L_2$  is in the region in which the deflection function  $\Theta(L)$  is near the Coulomb function. Because of this, one can set  $\Theta(L_2) \approx \Theta_C(L_2)$ , where the Coulomb deflection function  $\Theta_C(L)$  is expressed in terms of the Coulomb phase shift  $\sigma(L)$ :

$$\Theta_C(L) = 2 \frac{d\sigma(L)}{dL}, \quad 2\sigma(L) = i \ln \frac{\Gamma\left(L + \frac{1}{2} - i n\right)}{\Gamma\left(L + \frac{1}{2} + i n\right)},$$

and the Sommerfeld parameter  $n = Z_1 Z_2 e^2 m / \hbar k$ , where  $Z_1 e$  and  $Z_2 e$  are the charges of the colliding particles and  $m$  is their reduced mass. If the Coulomb interaction is sufficiently strong ( $n \gg 1$ ), then, using the asymptotic behavior of the gamma functions, we obtain

$$2\sigma(L) \approx 2\sigma(1/2) + n \ln \left( 1 + \frac{L^2}{n^2} \right) + 2L \tan^{-1} \frac{n}{L} + O\left(\frac{1}{n}\right).$$

Hence

$$\Theta_C(L) = 2 \tan^{-1}(n/L).$$

Since  $L_2$  is in the region in which the deflection function  $\Theta(L)$  is near the Coulomb function, we can assume  $L_2 = n \cot(\theta/2)$ .

We determine the critical angle on the grazing trajectory for Coulomb scattering:

$$\theta_c = \Theta_C(L_0) = 2 \tan^{-1}(n/L_0).$$

Then, noting that  $\Theta'(L_2) = -(2/n) \sin^2(\theta/2)$ , we obtain for the scattering amplitude the expression<sup>6</sup>

$$f(\theta) = f_c(\theta) \frac{1}{2} \operatorname{erfc} \left[ e^{-i\frac{\pi}{4}} \sqrt{\frac{L_0}{2 \sin \theta_c}} 2 \sin \frac{1}{2} (\theta - \theta_c) \right], \quad (21)$$

where the Rutherford scattering amplitude is

$$f_c(\theta) = -\frac{n}{2k \sin^2 \frac{\theta}{2}} \exp \left\{ 2i \left[ \sigma\left(\frac{1}{2}\right) - n \ln \sin \frac{\theta}{2} \right] \right\}.$$

The differential scattering cross section is determined by the square of the modulus of the amplitude (21). This result is the approximation of Fresnel diffraction for the scattering of heavy ions by nuclei.<sup>14</sup> Indeed, the ratio of the cross section to the Rutherford cross section is equal to the ratio of the intensity of the light scattered by the edge of a half-plane to the intensity of the incident light in optics if a light source is at a finite distance from the edge of a scattering half-plane [the error function  $\operatorname{erfc}(t)$  can be expressed in terms of Fresnel integrals]. Although in nuclear scattering the source of the particles is infinitely far from the target, the strong Coulomb field acts on a particle like a diverging lens, if the sign of the charge of the particle is equal to that of the charge of the nucleus, or a converging lens, if the signs of the charges are opposite. In this case, the action of the Coulomb field has the consequence that the incident particle is scattered by the nucleus in the same way as if it emerged from a virtual point source at a finite distance from the scattering center. Therefore, the conditions of Fraunhofer diffraction are replaced in the case of a strong Coulomb interaction by the conditions of Fresnel diffraction.<sup>15</sup> It should be noted that the amplitude (21) is a rough approximation describing only the qualitative aspect of the scattering. For the theoretical analysis of experimental data, it is necessary to use the exact expressions of Refs. 14 and 15.

The amplitude (21) is obtained under the assumption that  $L_2$  is not too close to  $L_r$  ( $L_2 > L_r$ ) and, accordingly,  $\theta$  is not very close to  $\theta_r$  ( $\theta < \theta_r$ ). If  $\theta$  approaches  $\theta_r$ , then it is again necessary to expand  $A_0^+(L, \theta)$  to terms of third order, since  $\Theta'(L_r) = 0$ . In this case, in the presence of strong absorption, we obtain

$$f(\theta) = \frac{1}{k} \sqrt{\frac{L_r}{2\pi \sin \theta}} \exp \left\{ i \left[ 2\delta(L_r) - L_r \theta - \frac{\pi}{4} \right] \right\} \\ \times \int_{L_0}^{\infty} dL \exp \left\{ i \left[ (\theta_r - \theta)(L - L_r) + \frac{1}{6} \Theta''(L_r)(L - L_r)^3 \right] \right\}.$$

We define the incomplete Airy function  $\text{Ai}(u, t)$  by means of the relation

$$\text{Ai}(u, t) = \frac{1}{2\pi} \int_t^{\infty} dx \exp \left[ i \left( xu + \frac{1}{3} x^3 \right) \right]. \quad (22)$$

Then the scattering amplitude and the cross section take the form<sup>6</sup>

$$f(\theta) = \frac{1}{k} \sqrt{\frac{2\pi L_r}{\sin \theta}} \exp \left\{ i \left[ 2\delta(L_r) - L_r \theta - \frac{\pi}{4} \right] \right\} \left[ \frac{2}{\Theta''(L_r)} \right]^{1/3} \\ \times \text{Ai} \left\{ \frac{\theta_r - \theta}{\left[ \frac{1}{2} \Theta''(L_r) \right]^{1/3}}, \left[ \frac{1}{2} \Theta''(L_r) \right]^{1/3} (L_0 - L_r) \right\}, \\ \sigma(\theta) = \frac{2\pi L_r}{k^2 \sin \theta} \left[ \frac{2}{\Theta''(L_r)} \right]^{2/3} \left| \text{Ai} \left\{ \frac{\theta_r - \theta}{\left[ \frac{1}{2} \Theta''(L_r) \right]^{1/3}}, \left[ \frac{1}{2} \Theta''(L_r) \right]^{1/3} \right. \right. \\ \left. \left. \times (L_0 - L_r) \right\} \right|^2. \quad (23)$$

To establish the behavior of the cross section (23), it is necessary to consider the properties of the incomplete Airy function  $\text{Ai}(u, t)$ . For  $t \rightarrow \pm \infty$ , we obtain  $\text{Ai}(u, -\infty) = \text{Ai}(u)$ ,  $\text{Ai}(u, \infty) = 0$ . The asymptotic behavior of  $\text{Ai}(u, t)$  for  $|u| \rightarrow \infty$  can be obtained by estimating the integral in (22) by the method of stationary phase.<sup>6</sup>

On the illuminated side of the rainbow ( $u < 0$ ), there are stationary points  $x = \pm \sqrt{-u}$ , and in the limit  $u \rightarrow -\infty$  we obtain

$$\text{Ai}(u, t) \approx \frac{1}{4} e^{i\frac{\pi}{4}} (-\pi^2 u)^{-\frac{1}{4}} \{ e^{-i\frac{2}{3}(-u)^{3/2}} \\ \times \text{erfc} [e^{-i\frac{\pi}{4}} (-u)^{\frac{1}{4}} [t - (-u)^{\frac{1}{2}}]] - i e^{i\frac{2}{3}(-u)^{3/2}} \\ \times \text{erfc} [e^{i\frac{\pi}{4}} (-u)^{\frac{1}{4}} [t + (-u)^{\frac{1}{2}}]] \}, \quad u \rightarrow -\infty.$$

On the dark side of the rainbow ( $u > 0$ ), there are the stationary points  $x = \pm i\sqrt{u}$ , and in the limit  $u \rightarrow \infty$  we find

$$\text{Ai}(u, t) \approx \frac{1}{4} (\pi^2 u)^{-\frac{1}{4}} e^{-\frac{2}{3}u^{3/2}} \text{erfc}(u^{\frac{1}{4}} t), \quad u \rightarrow \infty.$$

Taking these results into account, we see that in the presence of strong absorption the Coulomb rainbow has the following features. On the illuminated side  $\theta < \theta_r$  there are two "branches" corresponding to the two stationary points in (22) and leading, as in (17), to rainbow oscillations, which, however, are rapidly damped, since the branch near  $L_0$  decreases more rapidly than the other branch. On the dark side  $\theta > \theta_r$ , the exponential decrease of the rainbow cross section becomes even more rapid due to the absorption, since

$$\text{erfc}(w) \approx (\pi w^2)^{-\frac{1}{2}} e^{-w^2}, \quad w \rightarrow \infty.$$

Thus, the existence of a Coulomb rainbow point can have a particularly strong influence on the behavior of the heavy-ion scattering cross section in the region of its rapid decrease near  $\theta_c$ . This conclusion is confirmed by the study of the experimentally measured differential cross sections for the scattering of heavy ions.<sup>16</sup>

### 3. ELASTIC SCATTERING OF LIGHT IONS BY NUCLEI AT INTERMEDIATE ENERGIES

We now consider the elastic scattering of light ions by nuclei at energies  $E \gtrsim 100$  MeV. For the scattering of light ions, the Coulomb interaction is relatively small, and the real part of the nuclear potential is fairly deep (see, for example, Refs. 17–19). Therefore, the deflection function for the scattering of light ions in the region of intermediate energies always corresponds to the case of strong attraction. The deflection function  $\Theta(L)$  takes small positive values at large impact parameters for trajectories that do not pass through the region of strong attraction, while at impact parameters less than the critical value corresponding to a trajectory that grazes the surface of the nucleus  $\Theta(L)$  becomes negative, as it must be in the case of attraction. At sufficiently high energies, the deflection function has two extrema: a low positive maximum near  $L_0$  (Coulomb rainbow) and a fairly deep negative minimum at  $L_r < L_0$ , corresponding to passage through the interior region of the nucleus (nuclear rainbow). The Coulomb rainbow does not have a significant influence on the behavior of the differential elastic scattering cross sections of light ions. However, the nuclear rainbow does have a strong influence on the form of the differential cross sections owing to a certain transparency of the nucleus at small  $L$  characteristic of light-ion scattering. This fact is important, since the analysis of such cross sections makes it possible to obtain valuable information about the nature of the nuclear refraction of the scattered waves in the interior region of the nucleus.

Since in the case of the interaction of light ions with nuclei at energies of tens and hundreds of mega-electronvolts the Sommerfeld parameter is not large, the Fraunhofer scattering regime holds for light nuclei. Therefore, for the angular distributions of the elastic scattering cross sections of light ions at energies  $E \gtrsim 10$  MeV/nucleon well-defined diffraction oscillations are characteristic; they have an almost constant period determined by the limiting angular momentum  $L_0$  of the region of strong absorption, and the envelope of the maxima of these oscillations decreases with increasing scattering angle in accordance with an exponential law.<sup>20</sup> However, some experimental investigations of the elastic scattering of  $^3\text{He}$  nuclei<sup>21,22</sup> and  $^4\text{He}$  nuclei<sup>23–26</sup> at higher energies ( $E \gtrsim 25$ –30 MeV/nucleon) showed that in this case the differential cross sections measured in a sufficiently wide range of angles have appreciable deviations from Fraunhofer behavior. In the region of small scattering angles, well-defined diffraction oscillations are observed, as before. However, with increasing scattering angle there is first a gradual filling of the minima and a violation of the exponential law of decrease, so that there is formed in the cross section a fairly broad maximum on which are superimposed damped oscillations, and then, from a certain angle a rapid and smooth decrease of the cross section takes place. Such behavior of the cross sections is not entirely of a diffraction nature. Examination of the available experimental data

on the elastic scattering of  $^3\text{He}$  and  $^4\text{He}$  nuclei by different nuclei reveals the following features. At a given energy, the effect is more clearly expressed for scattering by lighter nuclei. With increasing mass number of the target nucleus, the region with the behavior of the cross section as described above is shifted to larger scattering angles; for scattering by sufficiently heavy nuclei, the effect is not observed at all and one observes only partial filling of the minima. In the case of scattering by the same target nuclei, the effect is not observed at low energies; then, at higher energies, it can be observed in the region of large scattering angles, and the characteristic region of angles is shifted with increasing energy toward small scattering angles.

This behavior of the differential cross sections of elastic scattering is a manifestation of rainbow scattering in the presence of strong absorption. Further experimental investigations showed that the damping of the Fraunhofer oscillations is observed at sufficiently high energies in the differential cross sections of scattering of other ions by nuclei, for example, deuterons (Ref. 27),  $^6\text{Li}$  (Refs. 19, 28, and 29), and even heavier ions.<sup>30-33</sup> It should be noted that such damping of the oscillations is not always due to rainbow scattering.<sup>11</sup> This question will be discussed in more detail below.

In many studies, differential cross sections of elastic scattering of light ions by nuclei having the nature described above were analyzed by means of the optical model. The results of such calculations show that the considered effect arises because of the strong refraction of the scattered waves by a fairly deep real (refracting) part of the optical potential. Such behavior of the cross sections is sometimes called *refractive* behavior.<sup>17</sup> Differential cross sections that exhibit features of refractive behavior are sensitive to the choice of the real part of the optical potential, the greatest sensitivity being in the region of large angles, where there are no diffraction oscillations. Therefore, the analysis of such cross sections makes it possible to obtain important information about the optical potentials and in a number of cases to eliminate the discrete ambiguity in the determination of the depth of the refractive part of the potential.<sup>25,26</sup> The high sensitivity of the cross sections to the choice of the potential made it possible to discuss various refinements in the form of its refractive part. For example, Goldberg<sup>34</sup> considered an optical potential with real part in the form of the square of the Woods-Saxon function, and also in the form of a sum of the Woods-Saxon potential and its second derivative. Both forms of potential improved the agreement between the calculated and measured cross sections. In Ref. 35, the real part of the optical potential was chosen in the form of a sum of a Woods-Saxon part and a correction in the form of a Fourier-Bessel series, in which the coefficients were determined by fitting the calculated cross section to the experimental data.

The differential cross sections of elastic scattering of  $^4\text{He}$  nuclei by nuclei in the considered region of energies were also analyzed on the basis of definite parametrizations of the  $S$  matrix that take into account the presence of strong nuclear absorption and the presence of refraction of the scattered waves.<sup>23,36</sup> Elastic scattering of 104-MeV  $\alpha$  particles by different nuclei was studied in Ref. 23. The differential cross sections of  $\alpha$ -particle elastic scattering by heavy nuclei, for which refractive behavior was not observed, were described

in Ref. 23 by means of the two different parametrizations of the  $S$  matrix that are usually employed in the diffraction model. However, the cross sections of  $\alpha$ -particle scattering by light nuclei, where refractive behavior did occur, could not be described in Ref. 23 on the basis of the simple parametrizations of the  $S$  matrix.

A theoretical analysis was made in Ref. 36 of the differential cross sections that exhibit refractive behavior for the elastic scattering of 141.7-MeV  $\alpha$  particles by  $^{40}\text{Ca}$  and  $^{90}\text{Zr}$  nuclei. It proved possible in Ref. 36 to describe the differential cross sections by means of an  $S$  matrix in the form

$$S(L) = \eta(L) \exp \{2i[\delta(L) + \sigma(L)]\},$$

where the modulus  $\eta(L)$  was chosen in the form

$$\eta(L) = \varepsilon + (1 - \varepsilon) \exp \left[ -\exp \left( \frac{L_0 - L}{\Delta_0} \right) \right],$$

$\delta(L)$  and  $\sigma(L)$  are the nuclear and Coulomb phase shifts, and  $L_0$ ,  $\Delta_0$ , and  $\varepsilon$  are, respectively, the limiting angular momentum of strong absorption, the diffuseness parameter of the nuclear surface in the angular momentum space, and the transparency parameter of the nucleus in the region of small  $L$ . For the real nuclear phase shift  $\delta(L)$  a fairly complicated parametrization suggested by calculations in the optical model was used. In the analysis of the experimental data in Ref. 36 it was found to be important to take into account the small transparency  $\varepsilon$  for partial waves with small angular momenta.

Thus, for the study of the scattering of light ions by nuclei at energies  $E \gtrsim 25$ –30 MeV/nucleon on the basis of a modeling of the  $S$  matrix the simple parametrizations of the  $S$  matrix usually employed in the diffraction model are inadequate. To study the damping of the Fraunhofer oscillations associated with the presence of strong nuclear refraction it is necessary to choose correctly the real part, responsible for the refraction, of the nuclear phase shift. In the calculations made in what follows, the real part is determined in the form of an expansion with respect to a complete set of functions, and this makes it possible, through analysis of the experimentally measured differential elastic scattering cross sections, to elucidate the behavior of the nuclear phase shift and the quantum deflection function corresponding to it.

We proceed from an expansion of the scattering amplitude in Legendre polynomials and write it in the form

$$f(\theta) = \frac{i}{2k} \sum_{l=0}^{\infty} (2l+1) [1 - \eta_l \exp \{2i(\delta_l + \sigma_l)\}] P_l(\cos \theta). \quad (24)$$

For the modulus  $\eta_1$  of the  $S$  matrix we shall in what follows choose a definite parametrization corresponding to the presence of strong absorption, and the real nuclear phase shift  $\delta_1$  will be determined in the form of a series expansion with respect to a complete set of functions.

For numerical calculations, it is convenient to separate in (24) the amplitude  $f_C(\theta)$  of the Coulomb scattering:

$$f(\theta) = f_C(\theta) + \frac{i}{2k} \sum_{l=0}^{\infty} (2l+1) e^{2i\sigma_l} [1 - \eta_l e^{2i\delta_l}] P_l(\cos \theta). \quad (25)$$

If we go over in (25) from summation to integration

and replace the Legendre polynomials by their asymptotic expression in terms of the Bessel function,

$$P_l(\cos \theta) \approx \sqrt{\frac{\theta}{\sin \theta}} J_0(L\theta), \quad L = l + \frac{1}{2} \gg 1, \quad (26)$$

$$0 \leq \theta < 2(\sqrt{2} - 1)\pi,$$

then we obtain the scattering amplitude in the form

$$f(\theta) = f_c(\theta) + \frac{i}{k} \sqrt{\frac{\theta}{\sin \theta}} \int_0^\infty e^{2i\sigma(L)} [1 - \eta(L) e^{2i\delta(L)}] J_0(L\theta) L dL.$$

This expression was used to study the nuclear rainbow effect in the scattering cross sections of  $^3\text{He}$  and  $^4\text{He}$  in Refs. 37 and 38.

The quantum deflection function  $\Theta(L)$ , which is an important characteristic of the scattering process in the semi-classical treatment, can be represented in the investigated case in the form

$$\Theta(L) = \Theta_N(L) + \Theta_C(L), \quad (27)$$

where the nuclear,  $\Theta_N(L)$ , and Coulomb,  $\Theta_C(L)$ , parts of the deflection function can be expressed in terms of the nuclear,  $\delta(L)$ , and Coulomb,  $\sigma(L)$ , phase shifts in accordance with the formulas

$$\Theta_N(L) = 2d\delta(L)/dL, \quad (28)$$

$$\Theta_C(L) = 2d\sigma(L)/dL \approx 2 \tan^{-1}(n/L). \quad (29)$$

The characteristic features of the differential cross sections of elastic scattering of light ions with energies  $E \geq 100$  MeV through sufficiently large scattering angles are determined by the behavior of the deflection function at small impact parameters. We therefore require a sufficiently accurate determination of  $\Theta(L)$  not only for  $L \geq L_0$  but also for trajectories that penetrate into the nucleus ( $L < L_0$ ).

For the modulus  $\eta(L)$  of the  $S$  matrix in the presence of strong absorption of the scattered waves we can use the parametrization

$$\eta(L) = 1 - (1 - \varepsilon) g(L, L_0, \Delta_0), \quad (30)$$

$$g(L, L_0, \Delta_0) = \left[ 1 + \exp\left(-\frac{L - L_0}{\Delta_0}\right) \right]^{-1}.$$

Allowance for the finite transparency  $\varepsilon$  of the nucleus for the partial waves with small angular momenta is important for the description and explanation of the behavior of differential cross sections that exhibit a manifestation of the nuclear rainbow.

As the basic expression for the real part of the nuclear phase shift  $\delta(L)$  one can take the parametrization

$$\delta(L) = \delta_0 g(L, L_1, \Delta_1), \quad (31)$$

which has been successfully used in a number of studies<sup>39-41</sup> of different cases of scattering of light and heavy ions by nuclei. However, the phase shift (31) does not enable one to describe cross sections in which the nuclear rainbow effect is manifested. Therefore, we determine the real part of the nuclear phase shift in the form of the expression<sup>37</sup>

$$2\delta(L) = \sum_{m=0}^{\infty} a_m \Delta_1^m \frac{d^m}{dL^m} g(L, L_1, \Delta_1). \quad (32)$$

Such an expansion is valid, since the function  $g(L, L_1,$

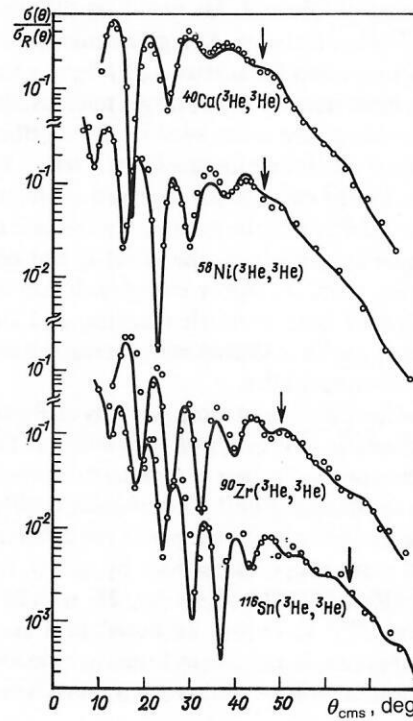


FIG. 4. Ratios of the differential cross sections of elastic scattering of 109.2-MeV  $^3\text{He}$  nuclei by nuclei to the Rutherford cross section. The experimental data are taken from Ref. 22.

$\Delta_1$ ) and all its derivatives together with unity form a complete system of functions,<sup>42</sup> with respect to which it is possible to expand an arbitrary function in the range of variation of  $L$  from zero to infinity. The expansion coefficients  $a_m$  in (32) can be determined by analyzing the experimentally measured differential cross sections of elastic scattering. Such a determination of the nuclear phase shift is analogous to a phase-shift analysis. In the calculations, the values of the parameters  $L_1$  and  $\Delta_1$  must be chosen in such a way that the series in (32) converges rapidly and a restriction can be made to the first few terms. In Ref. 43, an expansion of the type (32) was used for a model-free determination of the charge density in nuclei from an analysis of the differential

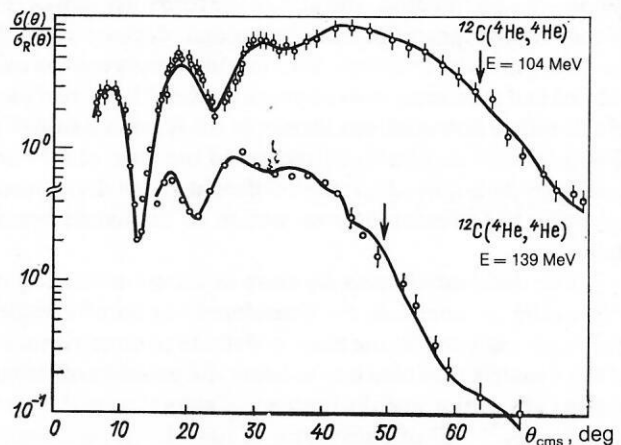


FIG. 5. Ratios of differential cross sections of elastic scattering of  $^4\text{He}$  nuclei by  $^{12}\text{C}$  nuclei to the Rutherford cross section. The experimental data are taken from Refs. 23 and 58.

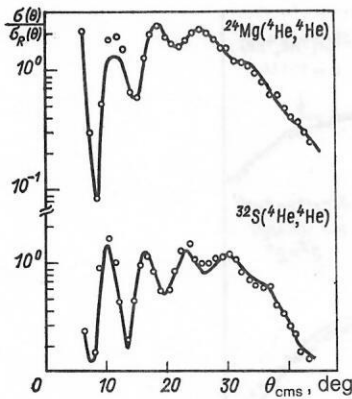


FIG. 6. Ratios of differential cross sections of elastic scattering of 166-MeV  $^4\text{He}$  nuclei by  $^{24}\text{Mg}$  and  $^{32}\text{S}$  nuclei to the Rutherford cross section. The experimental data are taken from Ref. 24.

cross sections of electron elastic scattering by nuclei.

The expressions (25), (30), and (32) provided the basis for an analysis of the differential cross sections of elastic scattering of  $^3\text{He}$  and  $^4\text{He}$  nuclei and also the heavier  $^6\text{Li}$  ions by different nuclei. The results of the calculations are shown together with the experimental points in Figs. 4–14. The values of the parameters used in the calculations are given in Table I. As can be seen from the figures, the calculated differential cross sections agree with the experimental data, correctly describing not only the diffraction oscillations at small angles but also the refractive behavior of the cross sections at large scattering angles. To achieve this agreement between the calculated and measured cross sections, 6–8 terms were retained in the expansion (32) of the nuclear phase shift (see Table I). The calculations confirm that the damping of the diffraction oscillations in the cross sections of elastic scattering of light ions by nuclei is due to the presence of strong nuclear refraction. Figure 15 gives as an example the modulus  $\eta(L)$  of the  $S$  matrix, the nuclear part  $2\delta(L)$  of the phase shift, and the quantum deflection function  $\Theta(L)$  calculated in accordance with (27)–(29) for the scattering of 141.7-MeV  $\alpha$  particles by  $^{40}\text{Ca}$  nuclei. It can be seen from Fig. 15 that the nuclear phase shift  $2\delta(L)$  reaches large values at small arguments and decreases smoothly with increasing  $L$ . The quantum deflection function  $\Theta(L)$  has a minimum at the angular momentum  $L_r = 14.5$ , which lies within the region of strong absorption. This minimum corresponds to the presence of a nuclear rainbow, and the corre-

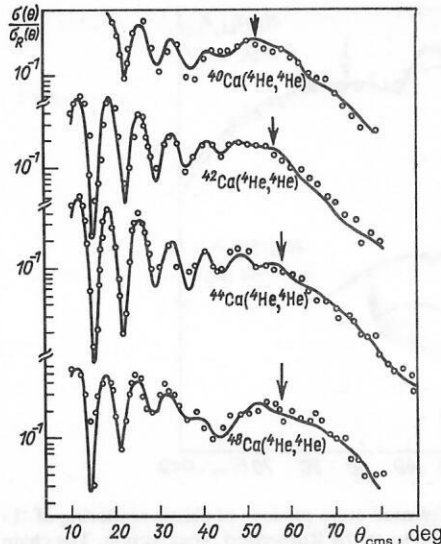


FIG. 8. Ratios of differential cross sections of elastic scattering of 104-MeV  $^4\text{He}$  nuclei by nuclei of the calcium isotopes to the Rutherford cross section. The experimental data are taken from Ref. 59.

sponding rainbow angle is  $\theta_r = 44^\circ$ . The nuclear part of the phase shift and the quantum deflection function in the remaining studied cases behave in the same way as shown for the corresponding quantities in Fig. 15. The values of the rainbow angles are given in Table I and are indicated by the arrows in the figures. It can be seen from the figures that the rainbow angles lie precisely in the region in which the differential cross section begins to decrease rapidly.

For qualitative understanding of the behavior of the studied differential cross sections, it is of interest to separate the contribution of the nuclear rainbow to them. The parametrization of the modulus  $\eta(L)$  of the  $S$  matrix in the form (30) makes it possible to divide the amplitude into two parts:

$$f(\theta) = ef_1(\theta) + (1 - e)f_2(\theta), \quad (33)$$

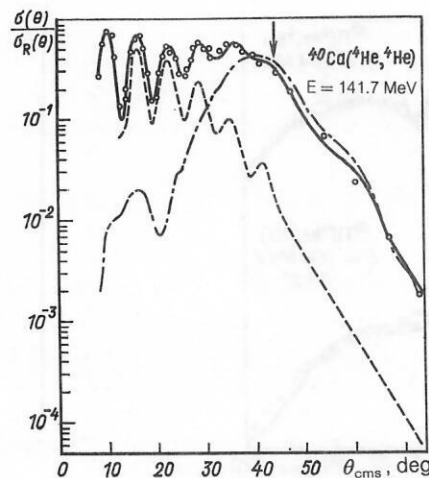


FIG. 9. Ratio of the differential cross section of elastic scattering of  $^4\text{He}$  nuclei by  $^{40}\text{Ca}$  nuclei to the Rutherford cross section. The chain curve and the broken curve are the ratios  $\sigma_1(\theta)/\sigma_R(\theta)$  (contribution of the nuclear rainbow) and  $\sigma_2(\theta)/\sigma_R(\theta)$  (see the text), respectively. The experimental data are taken from Ref. 17.

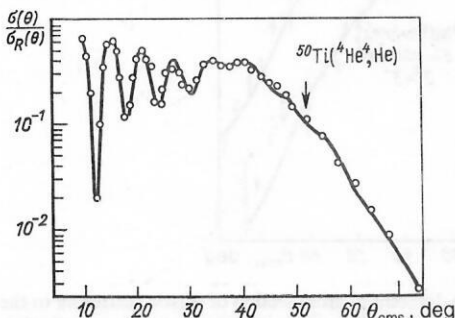


FIG. 7. Ratio of the differential cross section of elastic scattering of 140-MeV  $^4\text{He}$  nuclei by  $^{50}\text{Ti}$  nuclei to the Rutherford cross section. The experimental data are taken from Ref. 47.

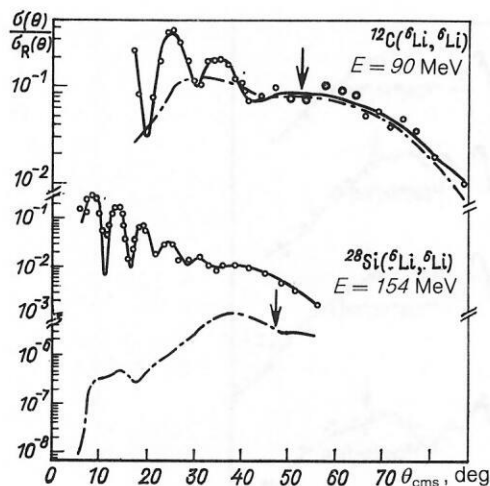


FIG. 10. Ratios of differential cross sections of elastic scattering of  ${}^6\text{Li}$  nuclei by  ${}^{12}\text{C}$  and  ${}^{28}\text{Si}$  nuclei to the Rutherford cross section. The chain curves show the contribution of the nuclear rainbow  $\sigma_1(\theta)/\sigma_R(\theta)$  (see the text). The experimental data are taken from Refs. 19 and 29.

where the amplitude  $f_1(\theta)$  corresponds to an  $S$  matrix with modulus  $\eta_1(L) = 1$ , and  $f_2(\theta)$  to an  $S$  matrix whose modulus  $\eta_2(L)$  is determined by the expression (30) with transparency  $\varepsilon = 0$ . The amplitude  $f_1(\theta)$  is due solely to the presence of refraction of the scattered waves and can be described by expressions analogous to (13) and (15). Therefore,  $f_1(\theta)$  is the rainbow scattering amplitude. The division of the amplitude (33) into two parts is meaningful if the point of the nuclear rainbow lies in the region of angular momenta in which the function  $\eta_2(L)$  is effectively equal to zero. Then the presence of the nuclear rainbow does not affect the behavior of the amplitude  $f_2(\theta)$ , which is determined by the strong absorption, the long-range nuclear interaction, and the nuclear refraction on the edge of the nucleus. Investigation of the behavior of amplitudes of the type  $f_2(\theta)$  shows that it is diffractive.<sup>7,11,36</sup> Moreover, the nearside,  $f_{2N}(\theta)$ , and farside,  $f_{2F}(\theta)$ , components of the

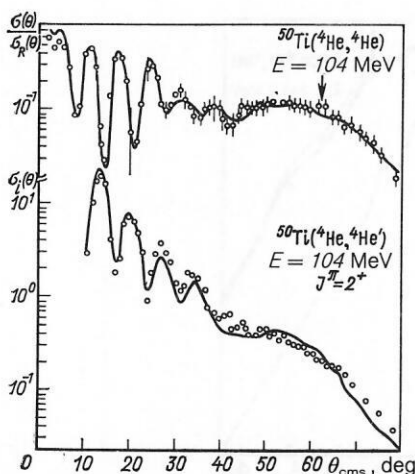


FIG. 11. Ratio of differential cross section of elastic scattering to the Rutherford cross section and the differential cross section (mb/sr) of inelastic scattering of  ${}^4\text{He}$  nuclei by  ${}^{50}\text{Ti}$  nuclei. In the inelastic scattering the  $2^+$  ( $E_2 = 1.56$  MeV) level of the titanium nuclei is excited. The experimental data are taken from Ref. 48.

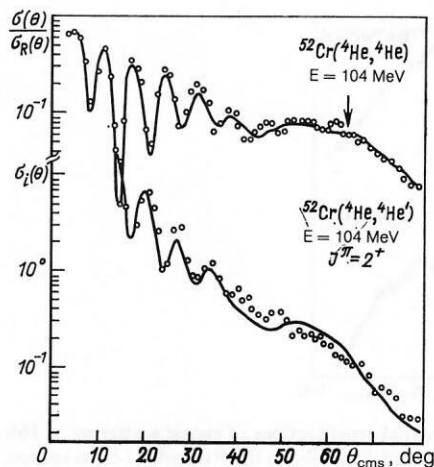


FIG. 12. Ratio of the differential cross section of elastic scattering to the Rutherford cross section and the differential cross section (mb/sr) of inelastic scattering of  ${}^4\text{He}$  nuclei by  ${}^{52}\text{Cr}$  nuclei. The  $2^+$  ( $E_2 = 1.43$  MeV) level of the chromium nuclei is excited in the inelastic scattering. The experimental data are taken from Ref. 48.

amplitude  $f_2(\theta)$  at sufficiently large angles  $\theta > \theta_0 = \theta(L_0)$  have Fraunhofer behavior:

$$f_{2F,N}(\theta) \sim (\sin \theta)^{-\frac{1}{2}} \exp(\pm iL_0\theta) \exp[-a_{F,N}(\theta \pm \theta_0)].$$

If we ignore the nuclear refraction on the edge of the nucleus, then the  $a_{F,N}$  smearing  $a_F = a_N = \pi\Delta_0$  of the nuclear surface. In this case, the nearside and farside amplitudes decrease with increasing angle in the same way, and their interference gives Fraunhofer oscillations of the cross section

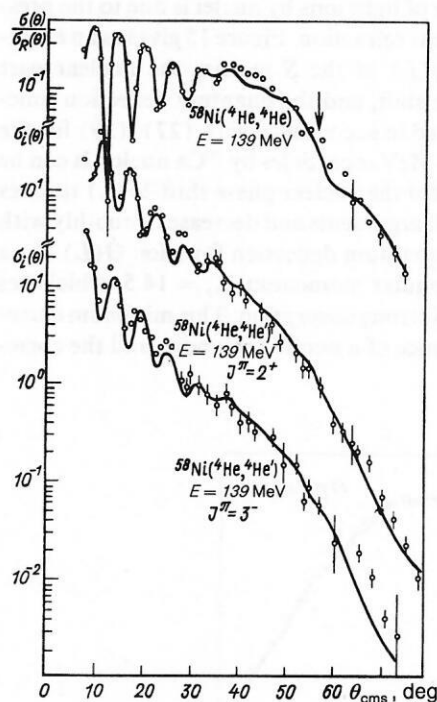


FIG. 13. Ratio of the differential cross section of elastic scattering to the Rutherford cross section and differential cross sections (mb/sr) of inelastic scattering of  ${}^4\text{He}$  nuclei by  ${}^{58}\text{Ni}$  nuclei. The  $2^+$  ( $E_2 = 1.45$  MeV) and ( $E_3 = 4.47$  MeV) levels of the nickel nuclei are excited in the inelastic scattering. The experimental data are taken from Ref. 26.

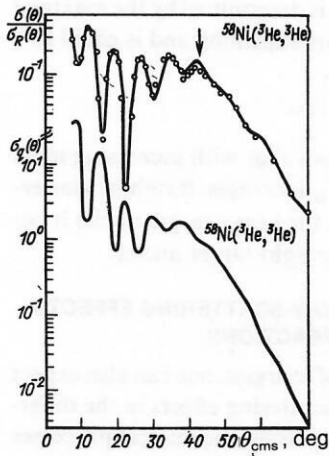


FIG. 14. Ratio of the differential cross section of elastic scattering of  $^3\text{He}$  nuclei to the Rutherford cross section (the experimental data are taken from Ref. 22) and the differential cross section (mb/sr) of the quasielastic ( $^3\text{He}, ^3\text{H}$ ) reaction at energy 118.5 MeV on  $^{58}\text{Ni}$  nuclei.

with period  $\pi/L_0$ . The existence of strong nuclear refraction on the edge of the nucleus has the consequence that  $a_F$  is less than  $a_N$ . Therefore, in the region of large scattering angles the amplitude  $f_{2F}(\theta)$  may become appreciably greater than  $f_{2N}(\theta)$ , and this leads to a damping of the Fraunhofer oscillations that is not due to the nuclear rainbow.<sup>11</sup>

Figure 9 illustrates the division of the amplitude into two contributions for elastic scattering of 141.7-MeV  $\alpha$  particles by  $^{40}\text{Ca}$  nuclei. Figure 9 gives the cross sections  $\sigma_1(\theta) = \varepsilon^2 |f_1(\theta)|^2$ ,  $\sigma_2(\theta) = (1 - \varepsilon)^2 |f_1(\theta)|^2$ , and  $\sigma(\theta) = |f(\theta)|^2$ . The cross section  $\sigma_1(\theta)$  has a purely rainbow nature and has a sharp peak near the rainbow angle  $\theta_r$ . It can be seen from Fig. 9 that the rainbow cross section

$\sigma_1(\theta)$  completely determines the behavior of the differential cross section in the region in which a broad maximum and rapid decrease of the cross section are observed. At small scattering angles, the diffraction contribution  $\sigma_2(\theta)$  is dominant. For  $\sigma_2(\theta)$ , constant exponential decrease with increasing scattering angle is characteristic. In the region of large angles we observe in  $\sigma_2(\theta)$  a damping of the Fraunhofer oscillations, which, as was noted above, is due to nuclear refraction on the edge of the nucleus. The contribution of the nuclear rainbow to the cross section depends strongly on the transparency parameter  $\varepsilon$ . For the scattering of heavy ions, the transparency for waves with small angular momenta is, as a rule, negligibly small, and the damping of the oscillations has the same form as in  $\sigma_2(\theta)$ . In this case, the damping of the diffraction oscillations is not a nuclear rainbow effect, though it is caused by nuclear refraction.<sup>11</sup> In this respect, the analysis of the differential cross sections of  $^6\text{Li}$  elastic scattering (see Fig. 10) is interesting. For scattering by  $^{12}\text{C}$  nuclei, the transparency parameter was found to be fairly large ( $\varepsilon = 0.083$ ), and the nuclear rainbow contribution  $\sigma_1(\theta)$  shown in Fig. 10 is dominant in the region of large scattering angles. In the case of scattering by  $^{28}\text{Si}$  nuclei, the transparency is small ( $\varepsilon = 0.00046$ ), so that the nuclear rainbow contribution is negligible at all scattering angles. It was noted in Ref. 19 that for the scattering of  $^6\text{Li}$  nuclei absorption stronger than for light nuclei is characteristic, and therefore the  $^6\text{Li}$  nucleus occupies an intermediate position between the light and the heavy ions. However, it should be noted that for a final conclusion about the manifestation or absence of the nuclear rainbow effect in the case of  $^6\text{Li}$  scattering by  $^{28}\text{Si}$  nuclei at energy 154 MeV the differential cross section must, if possible, be measured in a wider range of angles.<sup>44</sup>

We note that more recent investigations of elastic scat-

TABLE I. Table of parameters for calculating the differential cross sections of elastic scattering of  $^3\text{He}$ ,  $^4\text{He}$ , and  $^6\text{Li}$  nuclei by nuclei.

Incident nucleus	Target nucleus	Energy, MeV	$L_0$	$L_1$	$\Delta_0$	$\Delta_1$	$\varepsilon$	$a_0$	$a_1$	$a_2$	$a_3$	$a_4$	$a_5$	$a_6$	$a_7$	$\theta_r$ , deg	$\chi^2$
$^3\text{He}$	$^{40}\text{Ca}$	109.2	23.35	14.33	3.20	3.06	0.051	18.21	22.37	24.28	14.73	3.00	0.774	-0.510	-0.076	45	2.5
$^3\text{He}$	$^{58}\text{Ni}$	109.2	26.44	13.65	2.92	3.98	0.037	23.65	18.60	19.06	18.81	4.05	2.00	-0.185	-0.186	46	1.9
$^3\text{He}$	$^{90}\text{Zr}$	109.2	31.07	16.31	2.86	4.75	0.035	29.02	25.31	13.23	5.22	-7.13	-1.12	-1.46	-0.011	50	7.8
$^3\text{He}$	$^{116}\text{Sn}$	109.2	33.87	18.86	3.08	5.03	0.015	29.45	32.83	15.98	5.73	-7.40	-2.26	-1.56	-0.095	64	5.7
$^3\text{He}$	$^{58}\text{Ni}$	118.5	27.08	13.87	3.02	4.26	0.043	23.32	18.16	18.89	19.10	3.96	2.00	-0.169	-0.183	42	1.2
$^4\text{He}$	$^{12}\text{C}$	104	14.98	10.22	3.32	3.38	0.045	15.34	14.31	2.64	0.816	-1.93	-0.829	0.002	-0.120	63	1.6
$^4\text{He}$	$^{12}\text{C}$	139	17.24	12.25	2.09	3.46	0.086	12.73	11.94	2.53	1.19	-2.19	-0.450	-0.268	-0.008	49	1.6
$^4\text{He}$	$^{24}\text{Mg}$	166	25.63	16.27	2.83	4.09	0.091	14.58	9.62	6.94	2.03	-0.397	-0.053	—	—	40	1.0
$^4\text{He}$	$^{32}\text{S}$	166	28.25	19.82	3.32	3.97	0.035	14.81	11.49	7.14	1.65	-2.51	-0.889	0.063	—	46	1.0
$^4\text{He}$	$^{40}\text{Ca}$	104	25.67	16.56	2.23	4.13	0.068	23.03	23.96	17.78	4.26	-3.80	-1.51	-0.986	-0.066	52	1.1
$^4\text{He}$	$^{42}\text{Ca}$	104	26.24	15.32	2.58	4.39	0.045	25.18	24.52	7.96	5.29	-5.86	-1.22	-0.955	-0.081	57	7.0
$^4\text{He}$	$^{44}\text{Ca}$	104	26.83	14.89	2.52	4.28	0.039	27.76	25.38	12.17	5.77	-8.15	-2.07	-1.36	-0.175	57	7.1
$^4\text{He}$	$^{48}\text{Ca}$	104	27.69	16.80	3.11	4.34	0.097	20.18	19.80	10.75	2.16	-6.33	-0.724	-0.605	-0.169	57	3.1
$^4\text{He}$	$^{40}\text{Ca}$	141.7	29.57	18.94	3.46	4.97	0.078	21.55	20.09	11.94	8.50	1.38	-0.061	0.054	-0.048	44	0.9
$^4\text{He}$	$^{50}\text{Ti}$	104	27.54	16.91	3.37	3.9	0.066	21.31	24.09	19.72	9.77	-1.59	2.20	-0.580	0.222	62	2.4
$^4\text{He}$	$^{50}\text{Ti}$	140	30.93	19.84	2.60	4.35	0.061	22.17	20.02	16.72	11.93	2.29	1.67	0.383	0.164	52	1.1
$^4\text{He}$	$^{52}\text{Cr}$	104	27.85	16.75	3.41	3.65	0.064	21.63	23.41	24.49	9.66	-0.264	1.50	-0.568	0.191	64	2.1
$^4\text{He}$	$^{58}\text{Ni}$	139	32.02	22.59	3.32	4.74	0.026	22.71	26.95	13.82	8.33	-0.387	0.248	-0.255	0.033	56	2.3
$^6\text{Li}$	$^{12}\text{C}$	91	22.59	10.96	3.35	3.43	0.083	13.41	10.79	3.06	-0.509	-3.72	0.898	0.039	0.266	55	1.5
$^6\text{Li}$	$^{28}\text{Si}$	154	36.14	20.62	4.87	5.33	0.00046	21.87	21.87	15.33	3.76	0.177	0.556	-0.126	0.105	48	4.9

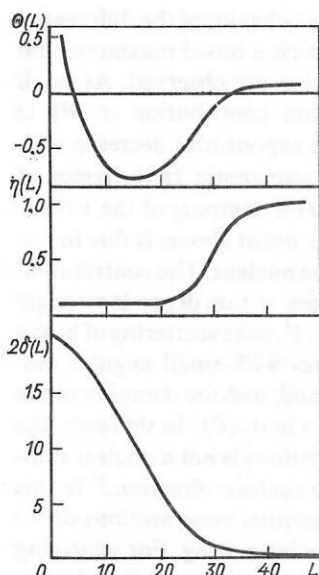


FIG. 15. Nuclear phase shift  $\delta(L)$ , deflection function  $\Theta(L)$ , and modulus  $\eta(L)$  of the  $S$  matrix as functions of the orbital angular momentum  $L = l + \frac{1}{2}$  for scattering of 141.7-MeV  ${}^4\text{He}$  nuclei by  ${}^{40}\text{Ca}$  nuclei.

tering of heavier ions by nuclei have shown that in the majority of cases the transparency is very small,  $\varepsilon < 10^{-4} - 10^{-5}$ , so that the nuclear rainbow effect is suppressed.<sup>11,45</sup> However, in some cases (for example, for the scattering of  ${}^9\text{Be}$  nuclei with energy 158 MeV by the light  ${}^{12}\text{C}$  and  ${}^{16}\text{O}$  nuclei<sup>30,45</sup>) the transparency is somewhat greater:  $\varepsilon \gtrsim 0.001$ . Such values of  $\varepsilon$  are small compared with the values characteristic of the scattering of light ions, but they still enable one to observe a weak manifestation of the nuclear rainbow in the differential cross sections. Although in these cross sections one does not observe the well-defined rainbow maximum seen in the scattering of light ions, one can nevertheless find a certain indication of the formation of such a maximum. Such behavior of the cross section has been dubbed the rainbow ghost.<sup>11,45</sup> In the scattering of  ${}^9\text{Be}$  nuclei with energy 158 MeV by  ${}^{26}\text{Mg}$  and heavier nuclei not even the rainbow ghost has been observed.<sup>45</sup>

Thus, if the nuclear rainbow effect is to be manifested there must be a certain transparency of the nucleus (a few percent) in the region of small angular momenta, and the deflection function  $\Theta(L)$  must have a minimum less than  $\pi$  in absolute magnitude. For scattering by the same target nuclei, the minimum of the deflection angle becomes deeper with decreasing energy and the rainbow angle increases, a conclusion that is confirmed by analysis of the experimental data (see Table I). At energies below a certain critical value, we have not a rainbow but orbiting at a point  $L = L_{\text{orb}}$ , so that  $\Theta(L_{\text{orb}}) = -\infty$ .<sup>4,5</sup> At such energies, the differential cross section will not exhibit rainbow scattering, but the behavior of the deflection function can be explained by means of the semiclassical expression (8). At not too large  $L$ , the effective potential  $U_{\text{ef}}(r) = U(r) + \hbar^2 L^2 / 2mr^2$  has on the boundary of the nucleus a barrier formed by the Coulomb and centrifugal potentials. But at large  $L$  the effective potential is a monotonically decreasing function of  $r$ . If the energy is not too high, then at a certain angular momentum  $L = L_{\text{orb}}$  the energy  $E$  is equal to the barrier, and the integral in (8) diverges. The critical energy  $E_{\text{cr}}$ , below which there is

orbiting and no rainbow point, is determined by the maximal height of the barrier in  $U_{\text{ef}}$  at its vanishing and is equal to<sup>25</sup>

$$E_{\text{cr}} = \left[ U(r) + \frac{r}{2} \frac{d}{dr} U(r) \right]_{\text{max}}.$$

Estimates of the energy  $E_{\text{cr}}$  show that with increasing mass number of the target nucleus  $E_{\text{cr}}$  increases. Rainbow scattering is observed at  $E > E_{\text{cr}}$ , i.e., for heavy target nuclei it occurs at higher energies than for light target nuclei.

#### 4. MANIFESTATION OF RAINBOW-SCATTERING EFFECTS IN QUASIELASTIC NUCLEAR REACTIONS

In the considered region of energies, one can also expect the manifestation of rainbow-scattering effects in the differential cross sections of various quasideastic nuclear processes that take place under conditions close to those of elastic scattering.

Indeed, experiments on the inelastic scattering of  ${}^3\text{He}$  (Ref. 46) and  ${}^4\text{He}$  (Refs. 26, 47, and 48) nuclei at energies  $E \gtrsim 25 - 30$  MeV/nucleon, and also of  ${}^6\text{Li}$  nuclei at energy  $E = 90$  MeV (Ref. 19) with excitation of low-lying collective states of the target nuclei, show that the differential cross sections of inelastic scattering also contain an effect of damping of the diffraction oscillations similar to the one described earlier for the elastic scattering cross sections. The damping of the oscillations in the inelastic cross sections occurs in the same region of angles as in the elastic ones.

In Ref. 26, inelastic scattering of 139-MeV  $\alpha$  particles with excitation of low-lying nuclear states was studied on the basis of the DWBA. The optical potential used in these calculations was deduced from analysis of the elastic scattering cross sections of  $\alpha$  particles of the same energy. The damping of the oscillations was described successfully in Ref. 26 both in the elastic and in the inelastic cross sections.

The approach developed in Sec. 3 can be generalized to a description on the basis of the adiabatic approximation for the differential cross sections of inelastic scattering with excitation of low-lying vibrational states of nuclei.

We shall proceed from the expression (25) for the elastic scattering amplitude. We replace the Legendre polynomials by their asymptotic expression in terms of a Bessel function in accordance with Eq. (26). Using for the Bessel functions the integral representation

$$J_m(L\theta) = \frac{(-i)^m}{2\pi} \int_0^{2\pi} \exp(iL\theta \cos \varphi + im\varphi) d\varphi,$$

we represent the scattering amplitude in the form

$$f(\theta) = f_c(\theta) + \frac{i}{2\pi k} \sqrt{\frac{\theta}{\sin \theta}} \sum_{l=0}^{\infty} \int_0^{2\pi} \exp(2i\sigma(L) + i\mathbf{b}\mathbf{q}) \times [1 - \eta(L) e^{2i\delta(L)}] L d\varphi, \quad (34)$$

where  $\mathbf{b}$  ( $\mathbf{b} = L/k$ ) and  $\mathbf{q}$  ( $\mathbf{q} = k\theta$ ) are two-dimensional vectors in the plane perpendicular to the direction of the incident beam, and  $\varphi$  is the angle between them.

We now consider small collective vibrations of the nuclear surface. We shall assume that the shape of the nucleus is determined by the expression

$$R(\vartheta, \varphi) = R \left[ 1 + \sum_{\lambda\mu} \alpha_{\lambda\mu} Y_{\lambda\mu}(\vartheta, \varphi) \right],$$

where  $R$  is the radius of the nucleus, and the  $z$  axis coincides

with the direction of the incident beam. The projection of the nucleus onto the plane perpendicular to the beam is

$$R(\varphi) = R \left[ 1 + \sum_{\lambda\mu} \alpha_{\lambda\mu} Y_{\lambda\mu} \left( \frac{\pi}{2}, \varphi \right) \right]. \quad (35)$$

Here, the quantities  $\alpha_{\lambda\mu}$  are related to the operators of creation,  $b_{\lambda\mu}^+$ , and annihilation,  $b_{\lambda\mu}$ , of surface phonons by

$$\alpha_{\lambda\mu} = \frac{\beta_\lambda}{\sqrt{2\lambda+1}} [b_{\lambda\mu} + (-1)^\mu b_{\lambda, -\mu}^\dagger],$$

where  $\beta_\lambda$  are the dynamical deformation parameters of the nucleus. The limiting angular momentum  $L_0$  is related to the radius  $R$  of the nucleus (the radius of strong absorption) by  $L_0 \approx kR$ . A similar relation holds for the parameter  $L_1$  if  $R$  is understood to be the radius of the refracting region of the nucleus. Therefore, to describe inelastic scattering with the excitation of surface vibrations in nuclei, we can replace the parameters  $L_0$  and  $L_1$  in accordance with (35):

$$L_{0,1}(\varphi) = L_{0,1} \left[ 1 + \sum_{\lambda\mu} \alpha_{\lambda\mu} Y_{\lambda\mu} \left( \frac{\pi}{2}, \varphi \right) \right].$$

Such a procedure is analogous to the one adopted in Ref. 53 to describe the cross sections of inelastic scattering of particles by nuclei. Expanding the integrand in (34) in a series in the small quantities  $\alpha_{\lambda\mu}$  up to the linear terms, we obtain

$$f(\theta) = f_e(\theta) + \sum_{\lambda\mu} \alpha_{\lambda\mu} f_{\lambda\mu}(\theta),$$

where the elastic scattering amplitude  $f_e(\theta)$  is determined by the expression (25), and the inelastic scattering amplitude  $f_{\lambda\mu}(\theta)$  is equal to

$$f_{\lambda\mu}(\theta) = \frac{i^{\mu+1}}{k} L_0 Y_{\lambda\mu} \left( \frac{\pi}{2}, 0 \right) \sqrt{\frac{\theta}{\sin \theta}} \times \sum_{l=0}^{\infty} L J_\mu(L\theta) \exp \{ 2i [\sigma(L) + \delta(L)] \} \times \left[ \frac{d\eta(L)}{dL} + 2i \frac{L_1}{L_0} \eta(L) \frac{d\delta(L)}{dL} \right]. \quad (36)$$

The expression (36) does not take into account the possibility of Coulomb excitation of the target nuclei, since the contribution of such a process to the cross section is small in the considered region of energies.<sup>49,50</sup>

We note that the expression (36) can also be obtained on the basis of the formalism developed in Ref. 51; this makes it possible to relate the inelastic scattering amplitude to the elastic amplitude by considering an optical potential deformed by small surface vibrations.

The differential cross section of inelastic scattering with excitation of low-lying single-phonon vibrational states with spin  $I$  in even-even nuclei is related to the amplitude (36) by

$$|\sigma_I(\theta)| = \frac{|\beta_I|^2}{2I+1} \sum_{M=-I}^I |f_{IM}(\theta)|^2.$$

To calculate the differential cross sections of the inelastic scattering of  $\alpha$  particles with energy 104 MeV by  $^{50}\text{Ti}$  and  $^{52}\text{Cr}$  nuclei and 139 MeV by  $^{58}\text{Ni}$  nuclei, we can use the results of analysis of the elastic scattering cross sections of  $\alpha$  particles of the same energies by the same nuclei (see Table I). The cross sections of inelastic scattering of  $\alpha$  particles by

$^{58}\text{Ni}$  nuclei were analyzed in Ref. 52 on the basis of the approach described above. Let us consider the scattering of  $\alpha$  particles with excitation of the  $2^+$  levels of the nuclei  $^{50}\text{Ti}$  ( $E_2 = 1.56$  MeV) and  $^{52}\text{Cr}$  ( $E_2 = 1.43$  MeV) and the  $2^+$  ( $E_2 = 1.45$  MeV) and  $3^-$  ( $E_3 = 4.47$  MeV) levels of  $^{58}\text{Ni}$  nuclei. The results of calculations of the differential cross sections of elastic and inelastic scattering together with the experimental data from Refs. 26 and 48 are given in Figs. 11–13. The dynamical-deformation parameters had the values  $|\beta_2| = 0.125$  for  $^{50}\text{Ti}$ ,  $|\beta_2| = 0.111$  for  $^{52}\text{Cr}$ , and  $|\beta_2| = 0.123$ ,  $|\beta_3| = 0.085$  for  $^{58}\text{Ni}$ . The functions  $\eta(L)$ ,  $\delta(L)$ , and  $\Theta(L)$  for all three nuclei behave like the functions shown in Fig. 15 and indicate the presence of a nuclear rainbow. As can be seen from Figs. 11–13, the calculated differential inelastic scattering cross sections of the  $\alpha$  particles agree with the experimental data. The value of  $\chi^2$  for the inelastic scattering cross sections is 2.3 for scattering by  $^{50}\text{Ti}$  nuclei, 2.0 for  $^{52}\text{Cr}$  nuclei, and 2.1 and 3.9 for  $^{58}\text{Ni}$  nuclei with excitation of the  $2^+$  and  $3^-$  levels respectively. In the region of the diffraction oscillations, the diffraction phase rule holds<sup>53</sup>: The cross section of inelastic scattering with excitation of single-phonon states of the nuclei oscillates in antiphase with the elastic scattering cross section if the spin of the final state of the even-even nuclei is even and in phase with it if the spin is odd. In the region of angles  $\theta \gtrsim \theta_r$ , the calculated differential cross sections of inelastic scattering correctly reproduce the observed damping of the diffraction oscillations.

Thus, correct choice of the nuclear phase shift  $\delta(L)$  makes it possible to describe by means of a single set of parameters the cross sections of elastic and inelastic scattering of light ions by nuclei at energies  $E \gtrsim 25$ –30 MeV/nucleon, for which the rainbow scattering effect is characteristic.

The manifestation of the nuclear rainbow in the cross sections of inelastic nuclear scattering with excitation of low-lying collective states of the target nuclei in the considered region of energies suggests that the nuclear rainbow will also occur in other quasielastic processes. These include, in particular, the ( $^3\text{He}$ ,  $^3\text{H}$ ) charge-exchange nuclear reaction, which is accompanied by excitation of the isobar analog of the ground state of the target nucleus.

We proceed from the expression (25) for the elastic scattering amplitude, in which the modulus  $\eta(L)$  of the  $S$  matrix and the nuclear phase shift  $\delta(L)$  have, as before, the form (30) and (32). To introduce an isospin part into the expression for the scattering amplitude, we use a procedure like the one employed in Refs. 54 and 55, and we replace the parameters  $L_0$  and  $L_1$  by

$$L_{0,1}(t, T) = L_{0,1} + \varepsilon_t t T,$$

where  $t$  and  $T$  are the operators of the isotopic spin of the incident particle and the target nucleus, respectively, and  $\varepsilon_t$  is a constant that characterizes the isospin part of the interaction. Expanding the scattering amplitude up to terms of first order in the small quantity  $\varepsilon_t$ , we obtain

$$f(\theta) = f_0(\theta) + f_t(\theta) t T,$$

where the amplitude  $f_0(\theta)$  is determined by the expression (25), and for the amplitude  $f_t(\theta)$  we obtain

$$f_t(\theta) = \frac{ie_t}{k} \sum_{l=0}^{\infty} L \exp \{ i [\sigma(L) + \sigma'(L) + 2\delta(L)] \} \times \left[ \frac{d\eta(L)}{dL} + 2i\eta(L) \frac{d\delta(L)}{dL} \right] P_l(\cos \theta). \quad (37)$$

In (37), we have taken into account the difference between the Coulomb phase shifts  $\sigma(L)$  and  $\sigma'(L)$  in the entrance and exit channels. The differential cross section of the ( $^3\text{He}$ ,  $^3\text{H}$ ) charge-exchange reaction with formation of the isobar analog of the target-nucleus ground state is related to the amplitude (37) by the expression

$$\sigma_q(\theta) = \frac{1}{4} (T+M)(T-M+1) |f_t(\theta)|^2,$$

where  $T$  and  $M$  are the isospin and isospin projection of the target nucleus.

The differential cross section of the quasielastic ( $^3\text{He}$ ,  $^3\text{H}$ ) charge-exchange reaction on the  $^{58}\text{Ni}$  nucleus at energy 118.5 MeV can be calculated by using the results of the analysis of the elastic scattering cross section of  $^3\text{He}$  nuclei at the same energy by the same nuclei (see Table I). For the parameter  $\varepsilon_r$ , which does not influence the shape of the cross section, the value  $\varepsilon_r = 0.1$  was taken. The results of the calculations of the differential cross sections of elastic scattering of  $^3\text{He}$  nuclei and the ( $^3\text{He}$ ,  $^3\text{H}$ ) reaction are given in Fig. 14, from which it can be seen that the cross section of the ( $^3\text{He}$ ,  $^3\text{H}$ ) charge-exchange reaction behaves in the same way as the elastic scattering cross section for  $^3\text{He}$  nuclei.<sup>38,56</sup> At small scattering angles we again observe in the calculated charge-exchange reaction cross section diffraction oscillations that satisfy a phase rule<sup>57</sup>: The cross section of the inelastic charge-exchange reaction oscillates in antiphase with the elastic scattering cross section. In the region of angles  $\theta \gtrsim \theta_r$  we observe damping of the oscillations and a subsequent rapid decrease of the ( $^3\text{He}$ ,  $^3\text{H}$ ) reaction cross section that has a rainbow nature.

Thus, our analysis shows that the rainbow scattering effect is characteristic not only of elastic scattering of light ions by nuclei but also of various quasi-inelastic processes in the same region of energies of the colliding particles.

## 5. CONCLUSIONS

The investigation of the processes of nuclear scattering in the region of intermediate energies shows that in many cases the angular distributions of the cross sections exhibit an effect analogous to rainbow scattering of light in optics. Thus, the theoretical analysis of the experimentally measured differential cross sections of elastic scattering of the light ions  $^3\text{He}$  and  $^4\text{He}$  by nuclei at energies  $E \gtrsim 100$  MeV confirms that the damping of the Fraunhofer oscillations with subsequent rapid smooth decrease of the cross section that is observed in this case presents a picture of rainbow scattering associated with a minimum of the corresponding quantum deflection function within the region of strong absorption  $L < L_0$  (nuclear rainbow). The occurrence of the nuclear rainbow in the elastic scattering cross sections is made possible by the fact that for the scattering of light ions the absorption is relatively small, so that there exists a certain transparency of the nucleus (a few percent) for partial waves with small angular momenta. Because of this, the analysis of such cross sections makes it possible to elucidate the nature of nuclear refraction in the interior region of the

nucleus, to determine more accurately the behavior of the optical potentials at short distances, and to determine the real part of the nuclear phase shift at small values of the orbital angular momentum.

Further investigations showed that rainbow scattering is also observed in the inelastic scattering of light ions with excitation of low-lying collective states of nuclei. The behavior of the differential cross section of these quasielastic processes can be described by using characteristics extracted from analysis of the elastic scattering cross section. This permits the conclusion that rainbow scattering must also be observed in other quasielastic nuclear processes. These include, in particular, the ( $^3\text{He}$ ,  $^3\text{H}$ ) charge-exchange reaction accompanied by excitation of the isobar analog of the state of the target nucleus. Calculations show that the cross section of such a reaction at energies  $E \gtrsim 100$  MeV does indeed present a picture of rainbow scattering. A final confirmation of this prediction can be obtained after appropriate experiments have been made.

For the scattering of heavy ions by nuclei, the absorption has, as a rule, a much larger value than in the case of light ions, and the transparency of the nucleus for partial waves with small angular momenta is negligibly small. This makes a manifestation of the nuclear-rainbow effect impossible in the interaction of heavy ions with nuclei. The damping of the Fraunhofer oscillations in the region of large scattering angles that is sometimes observed in the cross sections of heavy ions is to be attributed in the majority of cases to a specific effect of the nuclear refraction on the edge of the nucleus. In such cross sections, the characteristic broad rainbow maximum is absent. Analysis of such cross sections can give valuable information about the nuclear refraction in the boundary region of the nucleus. Another effect associated with nuclear refraction on the edge of the nucleus is the Coulomb rainbow. The Coulomb rainbow has a strong influence on the behavior of the differential cross sections of elastic scattering of heavy ions in the region of angles  $\theta \sim \theta_C$ , where a rapid decrease of the cross section is observed.

The phenomenon of rainbow scattering in nuclear collisions is much richer and more varied from the physical point of view than the rainbow in optics. For a deeper understanding of all the phenomena associated with the manifestation of rainbow scattering it will be necessary to make further systematic experimental investigations of elastic and inelastic nuclear processes and to interpret them theoretically.

<sup>1</sup>M. Lozzi, *Istoriya fiziki* (History of Physics, translated from Italian), Mir, Moscow (1970).

<sup>2</sup>H. M. Nussenzweig, *Sci. Am.* **236**, No. 4, 116 (1977).

<sup>3</sup>H. C. van de Hulst, *Light Scattering by Small Particles* (Wiley, New York, 1957) [Russian translation published by Izd. Inostr. Lit., Moscow (1961)].

<sup>4</sup>R. G. Newton, *Scattering Theory of Waves and Particles* (McGraw-Hill, New York, 1966) [Russian translation published by Mir, Moscow (1969)].

<sup>5</sup>K. W. Ford and J. A. Wheeler, *Ann. Phys. (N.Y.)* **7**, 259 (1959).

<sup>6</sup>W. E. Frahn, "Wave mechanics of heavy ion collisions," in: *Heavy-Ion, High Spin States and Nuclear Structure*, Vol. 1, Intern. Atomic Energy Agency, Vienna (1975), p. 157.

<sup>7</sup>N. Rowley and C. Marty, *Nucl. Phys.* **A266**, 494 (1976).

<sup>8</sup>W. E. Frahn and R. H. Venter, *Ann. Phys. (N.Y.)* **24**, 243 (1963).

<sup>9</sup>Yu. A. Berezhnoi and G. A. Khomenko, *Ukr. Fiz. Zh.* **24**, 1024 (1979).

<sup>10</sup>R. C. Fuller, *Phys. Rev. C* **12**, 1561 (1975).

<sup>11</sup>K. W. McVoy and G. R. Satchler, *Nucl. Phys.* **A417**, 157 (1984).

<sup>12</sup>J. Knoll and R. Schaeffer, *Ann. Phys. (N.Y.)* **97**, 307 (1976).

<sup>13</sup>R. M. Eisberg and C. E. Porter, *Rev. Mod. Phys.* **33**, 190 (1961).

<sup>14</sup>W. E. Frahn, *Nucl. Phys.* **75**, 577 (1966).

- <sup>15</sup>W. E. Frahn, *Ann. Phys. (N.Y.)* **72**, 524 (1972).
- <sup>16</sup>N. Alamanos, F. Auger, J. Barrette, *et al.*, *Phys. Lett.* **137B**, 37 (1984).
- <sup>17</sup>D. A. Goldberg, S. M. Smith, and G. F. Burdzik, *Phys. Rev. C* **10**, 1362 (1974).
- <sup>18</sup>M. Hyakutake, I. Kumabe, M. Fukada, *et al.*, *Nucl. Phys.* **A333**, 1 (1980).
- <sup>19</sup>Yu. A. Glukhov, A. S. Dem'yanova, S. I. Drozdov, *et al.*, *Yad. Fiz.* **34**, 312 (1981) [*Sov. J. Nucl. Phys.* **34**, 177 (1981)].
- <sup>20</sup>E. V. Inopin and Yu. A. Bereznoi, *Ukr. Fiz. Zh.* **7**, 343 (1962).
- <sup>21</sup>N. Willis, I. Brissaud, Y. Le Bornec, *et al.*, *Nucl. Phys.* **A204**, 454 (1973).
- <sup>22</sup>M. Hyakutake, M. Matoba, I. Kumabe, *et al.*, *Nucl. Phys.* **A311**, 161 (1978).
- <sup>23</sup>G. Hauser, R. Löhken, H. Rebel, *et al.*, *Nucl. Phys.* **A128**, 81 (1969).
- <sup>24</sup>T. Brissaud, Y. Le Bornec, B. Tatischeff *et al.* *Nucl. Phys.* **A191**, 145 (1972).
- <sup>25</sup>D. A. Goldberg and S. M. Smith, *Phys. Rev. Lett.* **29**, 500 (1972).
- <sup>26</sup>D. A. Goldberg, S. M. Smith, H. G. Pugh, *et al.*, *Phys. Rev. C* **7**, 1938 (1973).
- <sup>27</sup>E. J. Stephenson, C. C. Foster, P. Schwandt, and D. A. Goldberg, *Nucl. Phys.* **A359**, 316 (1981).
- <sup>28</sup>R. M. De Vries, D. A. Goldberg, J. W. Watson, *et al.*, *Phys. Rev. Lett.* **39**, 450 (1977).
- <sup>29</sup>P. Schwandt, S. Kailas, W. W. Jacobs, *et al.*, *Phys. Rev. C* **21**, 1656 (1980).
- <sup>30</sup>G. R. Satchler, C. B. Fulmer, R. L. Auble, *et al.*, *Phys. Lett.* **128B**, 147 (1983).
- <sup>31</sup>M. E. Brandan, *Phys. Rev. Lett.* **49**, 1132 (1982).
- <sup>32</sup>H. E. Bohlen, M. R. Clover, G. Ingold, *et al.*, *Z. Phys. A* **308**, 121 (1982).
- <sup>33</sup>M. Buenerd, P. Martin, R. Bertholet, *et al.*, *Phys. Rev. C* **26**, 1299 (1982).
- <sup>34</sup>D. A. Goldberg, *Phys. Lett.* **55B**, 59 (1975).
- <sup>35</sup>E. Friedman and C. J. Batty, *Phys. Rev. C* **17**, 34 (1978).
- <sup>36</sup>S. K. Kauffmann, *Z. Phys. A* **282**, 163 (1977).
- <sup>37</sup>Yu. A. Bereznoi and V. V. Pilipenko, *Ukr. Fiz. Zh.* **27**, 177 (1982).
- <sup>38</sup>Yu. A. Bereznoi and V. V. Pilipenko, in: *Problemy yadernoi fiziki i kosmicheskikh lucheĭ* (Problems of Nuclear Physics and Cosmic Rays), No. 19, Khar'kov State University (1983), p. 3.
- <sup>39</sup>J. A. McIntyre, K. H. Wang, and L. C. Becker, *Phys. Rev.* **117**, 1337 (1959).
- <sup>40</sup>J. Alster, *Phys. Rev.* **141**, 1138 (1966).
- <sup>41</sup>W. E. Frahn and K. E. Rehm, *Phys. Rep.* **37C**, 2 (1978).
- <sup>42</sup>B. I. Tishchenko and E. V. Inopin, *Yad. Fiz.* **7**, 1029 (1968) [*Sov. J. Nucl. Phys.* **7**, 618 (1968)].
- <sup>43</sup>V. K. Luk'yanov, I. Zh. Petkov, and Yu. S. Pol', *Yad. Fiz.* **9**, 349 (1969) [*Sov. J. Nucl. Phys.* **9**, 204 (1969)].
- <sup>44</sup>A. S. Dem'yanova, Preprint 4139/2 [in Russian], I. V. Kurchatov Institute of Atomic Energy, Moscow (1985).
- <sup>45</sup>C. B. Fulmer, G. R. Satchler, K. A. Erb, *et al.*, *Nucl. Phys.* **A427**, 545 (1984).
- <sup>46</sup>C. J. Marchese, N. M. Clarke, and R. J. Griffiths, *Nucl. Phys.* **A202**, 421 (1973).
- <sup>47</sup>P. L. Roberson, D. A. Goldberg, N. S. Wall, *et al.*, *Phys. Rev. Lett.* **42**, 54 (1979).
- <sup>48</sup>R. Pesi, H. J. Gils, H. Rebel, *et al.*, *Z. Phys. A* **313**, 111 (1983).
- <sup>49</sup>W. H. Bassichis and A. Dar, *Ann. Phys. (N.Y.)* **36**, 130 (1966).
- <sup>50</sup>S. Varma and A. Dar, *Ann. Phys. (N.Y.)* **39**, 435 (1966).
- <sup>51</sup>N. Austern and J. S. Blair, *Ann. Phys. (N.Y.)* **33**, 15 (1965).
- <sup>52</sup>Yu. A. Bereznoi and V. V. Pilipenko, *Izv. Akad. Nauk SSSR Ser. Fiz.* **43**, 2240 (1983).
- <sup>53</sup>J. S. Blair, *Phys. Rev.* **115**, 928 (1959).
- <sup>54</sup>A. Y. Abul-Magd, *Nucl. Phys.* **A93**, 321 (1967).
- <sup>55</sup>W. E. Frahn, *Nucl. Phys.* **A107**, 129 (1968).
- <sup>56</sup>Yu. A. Bereznoi and V. V. Pilipenko, *Dokl. Akad. Nauk Ukr. SSR Ser. A*, No. 5, 52 (1984).
- <sup>57</sup>J. S. Blair, in: *Proc. of the Conf. on Direct Interactions and Nuclear Reaction Mechanisms*, Padua, September 3-8, 1962 edited by E. Clemental and G. Villi (Gordon and Breach, New York 1963), p. 669.
- <sup>58</sup>S. M. Smith, G. Tibell, A. A. Cowley, *et al.* *Nucl. Phys.* **A207**, 273 (1973).
- <sup>59</sup>H. J. Gils, E. Friedman, H. Rebel, *et al.*, *Phys. Rev. C* **21**, 1239 (1980).

Translated by Julian B. Barbour